

Preparation of Cerium Doped Cu/MIL-53(Al) Catalyst and Its Catalytic Activity in CO Oxidation Reaction

TAN Haiyan¹, ZHOU Yin², YAN Yunfan², HU Weibing¹, SHI Xinyu¹,
TAN Zhidou¹, TIAN Li¹, ZHENG Yin¹

(1. School of Chemistry and Environmental Engineering, Hubei University for Nationalities, Enshi 445000, China;
2. Sustainable Energy Laboratory, Faculty of Material Science and Chemistry, China University of Geosciences, Wuhan 430074, China)

Abstract: Metal-organic framework (MOF) material MIL-53(Al) with high thermal stability was prepared by a solvothermal method, serving as a support material of cerium doped copper catalyst (Ce-Cu)/MIL-53(Al) material for CO oxidation with high catalytic activity. The catalytic performance between the (Cu-Ce)/MIL-53(Al) and the Cu/MIL-53(Al) catalytic material was compared to understand the catalytic behavior of the catalysts. The catalysts were characterized by thermogravimetric-differential scanning calorimetry (TG-DSC), N₂ adsorption-desorption, X-ray diffraction (XRD), and transmission electron microscopy (TEM). The characterization results showed that MIL-53(Al) had good stability and high surface areas, the (Ce-Cu) nanoparticles on the MIL-53(Al) support was uniform. Therefore, the heterogeneous catalytic composite materials (Ce-Cu)/MIL-53(Al) catalyst exhibited much higher activity than that of the Cu/MIL-53(Al) catalyst in CO oxidation test, with 100% conversion at 80 °C. The results reveal that (Cu-Ce)/MIL-53(Al) is the suitable candidate for achieving low temperature and higher activity CO oxidation catalyst of MOFs.

Key words: metal-organic framework; solvothermal synthesis; MIL-53(Al); cerium doped copper catalyst; CO catalytic oxidation

1 Introduction

The oxidation reaction of CO is the basal issue in the catalysis field due to its theoretical and practical value^[1]. One of the key elements of the oxidation reaction is the development of active and stable catalysts with excellent catalytic performance. Recently, metal nanoparticles such as Au, Pd^[2,3] *etc* have been contributed to tackle these issues for delivering excellent performance for CO catalysts. However, due to the trend of particle agglomeration and thus corresponding drop of the specific surface area, these metal catalysts are easily deactivated. Consequently, developing low-cost catalysts with well-distributed form without serious agglomeration for application in selective CO oxidation is highly desirable.

Unlike traditional Au, Pd metal nanoparticles, metal-organic frameworks (MOFs) have been surveyed for their possible roles in catalytic applications owing

to their high pore volume, large surface area, geometrical control and varied nano structure controlled by a self-assembly process^[4-8]. The mechanically robust walls of the frameworks can be employed both to confine metal nanoparticles and to depress their growth, which are critical features to their applications in CO catalytic oxidation. Generally, catalysis based on MOFs include cyanosilylation of benzaldehyde and acetone^[9], oxidation of alkanes, olefins, alcohols, and amines^[10-15], hydroxylation of aromatic compounds^[16], hydrolysis of esters, esterification of acetic acid with 1-propanol^[17], and regioselective ring opening of epoxides^[18]. However, most of these MOFs catalyzed reactions are in liquid phase^[19], probably due to their stability limitation since most MOFs decompose at approximately 350 °C, which limits their catalytic application. In addition, MOFs' application in CO catalysis has also been impeded by their hardly accessible open-metal sites which are rather necessary in catalysis. Recently, (Al(OH)[O₂C-C₆H₄-CO₂]), one of the most studied MOFs and often denoted as MIL-53(Al), was used as a support material for catalyst in CO oxidation reaction. Compared with other MOFs carriers with nanoparticles, MIL-53(Al) as an excellent carrier with unique microporous structure and excellent thermal stability (550 °C) exhibits good catalytic performance^[3,20]. In particular,

©Wuhan University of Technology and SpringerVerlag Berlin Heidelberg 2017

(Received: May 30, 2015; Accepted: Nov. 4, 2016)

TAN Haiyan(谭海燕): Ph D; E-mail: Jftanhaiyan@sina.com

*Corresponding author: HU Weibing(胡卫兵): Prof.; Ph D;
E-mail: chemistryhu@126.com

Funded by the Guiding Research Project of Hubei Province
Department of Education (No. B2016098)

Tan *et al.*^[1] found that the conversion on Co/MIL-53(Al) was 100% at 160-180 °C. Liang *et al.*^[3] found that the conversion on Pd/MIL-53(Al) was 100% at 120-140 °C. But Jiang *et al.*^[2] reported the temperature for 100% oxidation of CO on Au/ZIF-8 at 315-340 °C before this. Obviously MIL-53(Al) as a carrier with good thermal stability showed excellent catalytic performance compared with ZIF-8 carrier. However, the temperature is relatively higher than that of traditional CO oxidation catalyst^[21-24].

Herein, based on Cu/MIL-53(Al) catalyst, we report the rational design and facile synthesis of cerium doped Cu/MIL-53(Al) catalyst (denoted by (Ce-Cu)/MIL-53(Al))^[20]. Obviously, the highly dispersed CeO₂ nanoparticles can limit the migration and aggregation of CuO nanoparticles, which will dramatically increase the activity in catalytic reactions. Also, cerium oxide owns the properties of N type semiconductors because they can easily transform valence between trivalent and tetravalent oxide, which encourages to excellent ability of storing and releasing oxygen. In addition, the thermal stability of the carrier, the sulfur storage capacity of the catalyst and the resistance to carbon deposit on catalysts are also improved remarkably. By doping cerium on the Cu/MIL-53(Al), the catalytic activity of the designed (Ce-Cu)/MIL-53(Al) material was remarkably enhanced comparing with that of Cu/MIL-53(Al).

2 Experimental

2.1 Preparation of catalyst

2.1.1 Materials

All reagents were obtained from standard suppliers and were analytical grade unless noted. Aqueous solutions were prepared with distilled water.

2.1.2 Synthesis of support MIL-53(Al)

Terephthalic acid (0.01 mol, 1.66 g) and Al(NO₃)₃·9H₂O (0.01mol, 3.75 g) were dissolved in 60 mL solvent (N,N-dimethylformamide (DMF): H₂O: =5:1, v/v). The resultant solution was stirred for 0.5 h and placed in a stainless steel vessel, which was sealed and placed in a programmable furnace. The mixture was heated to 220 °C at 5 °C·min⁻¹ and held at that temperature for 96 h, then cooled to room temperature. The products were filtered, washed with deionized water (4 × 15 mL) and ethanol (4 × 15 mL), and then air-dried to give 2.522 g of MIL-53(Al).

2.1.3 Synthesis of Cu/MIL-53(Al) catalyst and Ce doped Cu/MIL-53(Al) catalyst

Cu/MIL-53(Al) catalysts with different copper

loadings (5 wt%, 10 wt%, 15 wt%) were prepared by means of incipient wetness impregnation method of the respective MIL-53(Al) with the desired amount of aqueous copper nitrate. The wet mass was dried at 120 °C for 12 h. The samples were labeled as x%Cu/MIL-53(Al), in which *x* represents the copper loading. Ce doped Cu/MIL-53(Al) catalyst with 5 wt% cerium loading was prepared similarly.

2.2 Characterization of support and catalyst

TG-DSC analysis was performed with a NETZSCH STA449F3 analyzer in a temperature range of 30 to 600 °C in flowing O₂ with a heating rate of 10 °C·min⁻¹.

Prior to analysis the sample was first dried at 120 °C for 4 h. A Bruker advanced D8 powder X-ray diffractometer with monochromatic Cuka radiation and nickel filter equipped with VANTEC-1 detector was used for XRD measurements, the large angle scan ranges were 10-80°. N₂ adsorption-desorption experiment was conducted at -196 °C with a Quantachrome Autosorb-1-c/TCD/MS. The surface area was obtained from the adsorption branch by means of the BET model in relative pressure ranging from 0.05 to 0.3. The total pore volumes were calculated from the amount of N₂ vapor adsorbed at relative pressure of 0.99. TEM analyses of the samples were performed with an FEI TECNAI G2 F20 S-Twin microscope. X-ray photoelectron spectroscopy (XPS) analyses were performed on a VG Multilab 2000 spectrometer with Alka(1 486.6 eV) radiation. The binding energy was calibrated against the C1s peak (284.6 eV) of surface adventitious carbon.

2.3 Catalysis measurements

The CO catalytic oxidation activity was determined by using a fixed bed plug flow reactor system equipped with an on-line GC. Typically, pure CO and atmosphere were supplied through mass flow controllers and mixed with each other, and then the final reactant gas (800 mL·min⁻¹) was passed through the catalyst bed (1.0 g). Reaction gas was composed of CO (1 vol%) and atmosphere (37.5 vol%) and the gas hourly space velocity (GHSV) was 48 000 mL·h⁻¹·g⁻¹. The reaction temperature was programmed and controlled by means of thermocouple that extend to the catalyst bed inside the reactor. Heating rate of 2 °C·min⁻¹ was used to reach pre-set reaction temperature and the product gas was analyzed after 20 minutes of reaction at the set temperature. Reaction gas composition was monitored through on-line sampling using computer controlled Agilent Micro GC 3000A. The analysis was done after every 6 minutes of reaction time. CO conversion was calculated as follows.

$$\text{CO conversion} = \frac{([\text{CO}]_1 - [\text{CO}]_2)}{[\text{CO}]_1} \times 100$$

where $[\text{CO}]_1$ and $[\text{CO}]_2$ are inlet and outlet gas concentrations in ppm respectively. Prior to measurement the samples were first calcined at 400 °C for 4 h.

3 Results and discussion

3.1 TG-DSC result

The TG/DSC curve of the MIL-53(Al) carrier is shown in Fig.1. The TG curve shows that there is a continuous mass loss totaled 10% from room temperature to 500 °C due to the loss of physisorbed H₂O and residual ethanol in the MIL-53(Al) channels and the weight loss from 500 to 560 °C corresponds to the decomposition of BTC ligand (about 50%). In contrast, MIL-53(Al) shows better stability compared with most other metal organic frameworks decomposed at 350 °C^[20], which is beneficial to CO catalytic oxidation. The TG/DSC curve shows that the activation of the MIL-53(Al) sample is beneficial to its catalytic activity.

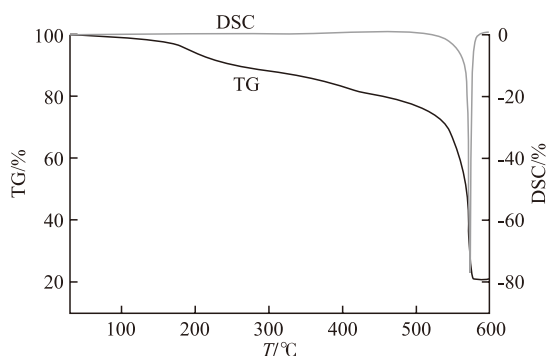


Fig.1 Thermogravimetric-differential scanning calorimetric(TG-DSC) curves of support MIL-53(Al)

3.2 N₂ adsorption-desorption result

The N₂ adsorption-desorption isotherms of MIL-53(Al) and (Cu-Ce)/MIL-53(Al) with various Cu/Ce ratios are shown in Fig.2. The curve shows a high specific surface area of the obtained MIL-53(Al) with 1 050 m²·g⁻¹. These curves are type IV(H₂) hysteresis loop, type of mesoporous silica with large cages and small opening pores. With increasing cerium-copper loading, the specific surface area of (5%Ce-5%Cu)/MIL-53(Al), (5%Ce-10%Cu)/MIL-53(Al) and (5%Ce-20%Cu)/MIL-53(Al) fell significantly to 780, 590 and 280 m²·g⁻¹ respectively, which indicates that cerium-copper species were introduced into the cages. It is reported that the size of the carrier specific surface area would greatly influence the activity of the catalyst, the bigger the specific surface area, the better the catalytic

activity^[1]. It is noticeable that the specific surface areas of the three compounds are obviously higher than that of traditional Ce-Cu catalyst^[25, 26], which implies more outstanding catalytic activation.

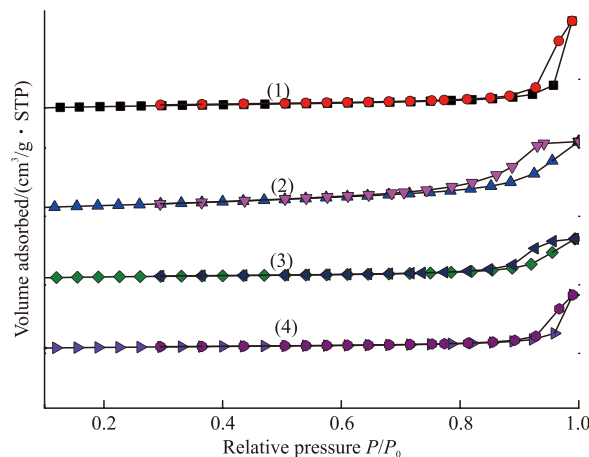


Fig.2 N₂ adsorption-desorption isotherms of the supports MIL-53(Al) and the corresponding catalysts: (1) MIL-53(Al), (2) (5%Ce-5%Cu)/MIL-53(Al), (3) (5%Ce-10%Cu)/MIL-53(Al), (4) (5%Ce-20%Cu)/MIL-53(Al)

3.3 TEM result

The morphology and structure of the MIL-53(Al) support and (Ce-Cu)/MIL-53(Al) catalyst are illustrated by TEM in Figs.3(a)-(d). The average particle sizes of MIL-53(Al) support are nearly 50 nm with uniform distribution (Fig.3(a)). The TEM images also indicate that the porous crystals are made of nanorods connected by such bridges, which can be observed at the edge of the particles (Figs.3(a)-(d)). For (Ce-Cu)/MIL-53(Al), there are no apparent aggregated particles, which implies that

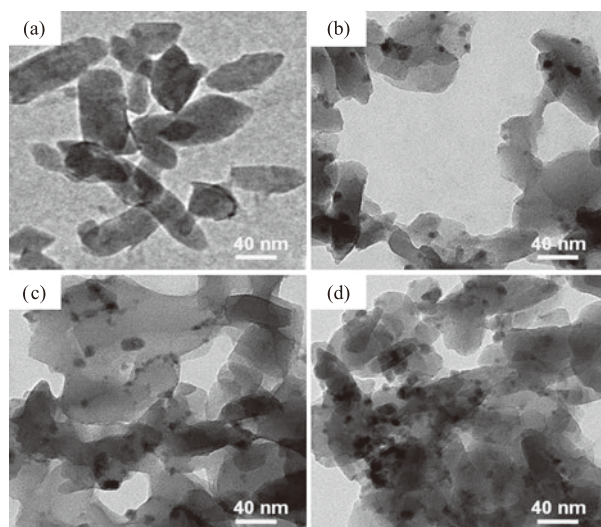


Fig.3 TEM of the supports MIL-53(Al) and the corresponding catalysts: (a) MIL-53(Al); (b) (5%Ce-5%Cu)/MIL-53(Al); (c) (5%Ce-10%Cu)/MIL-53(Al); (d) (5%Ce-20%Cu)/MIL-53(Al)

the (Ce-Cu) nanoparticles are well-distributed on the external surface of MIL-53(Al) support (Figs.3(b)-(d)). The well-size-distributed Ce-Cu nanoparticles, which resulted from the three dimensional porous structure of MIL-53(Al), give rise to a superior catalytic activity for CO oxidation.

3.4 XRD result

Fig.4 demonstrates that the X-ray diffraction (XRD) patterns of CeO₂ and CuO match well with the published powder XRD patterns. It is obvious that diffraction peaks at $2\theta=34.0^\circ$, 38.3° and 67.1° indicate that copper is present in the form of CuO crystalline phase on all the catalysts after calcination at 400 °C, which also means that most of the copper species were impregnated into the cages^[20]. From the XRD data, diffraction peaks at 28.5° , 47.7° and 56.8° are clearly observed. This result suggests the existence of cubic fluorite type of CeO₂, which can also be compared with the experimental pattern of crystalline CeO₂ nanoparticles^[27].

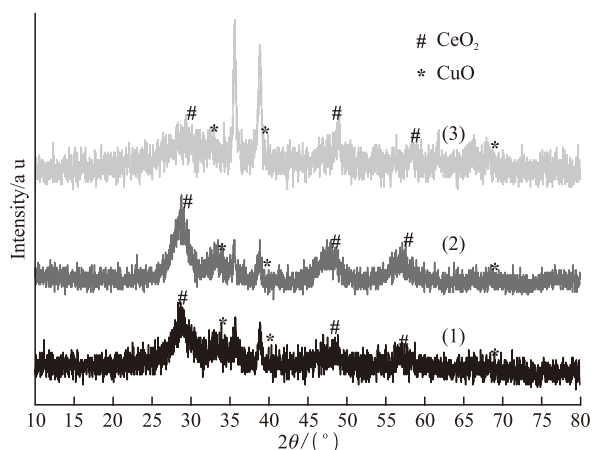


Fig.4 XRD patterns of support and catalysts: (1) (5%Ce-5%Cu)/MIL-53(Al), (2) (5%Ce-10%Cu)/MIL-53(Al), (3) (5%Ce-20%Cu)/MIL-53(Al)

3.5 XPS result

The Cu 2*p* core level spectrum of (Ce-Cu)/MIL-53(Al) catalysts is shown in Fig.5(a). The spectrum demonstrates that Cu is divalent copper ions because the binding energies at 952.33 eV and 932.06 eV are characteristic peaks for Cu²⁺^[18]. Especially, the binding energy is rather low and the ability of oxidation is extremely strong, which further confirms that Cu²⁺ is easy to catch oxygen atom for CO catalytic oxidation. For Ce 3*d* core level spectrum of (Ce-Cu)/MIL-53(Al) in Fig.5(b), the consisting of three peaks at 888.46, 916.53 and 906.98 eV corresponded to Ce⁴⁺ final states, while two possible peaks 882.25 and 900.61 eV are related to Ce³⁺ final states, which is consistent with previous reports^[28-30].

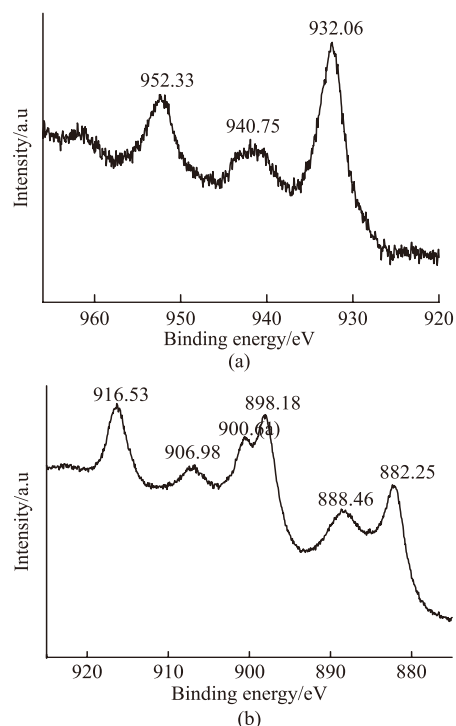


Fig.5 XPS spectra of (a) Cu and (b) Ce

3.6 Catalytic activity result and mechanism

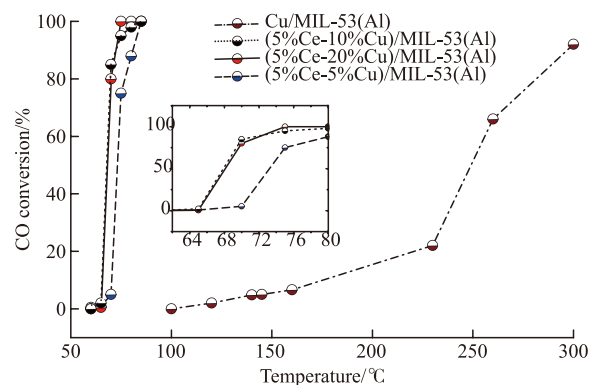


Fig.6 Catalytic performances of Cu/MIL-53(Al), (5%Ce-5%Cu)/MIL-53(Al), (5%Ce-10%Cu)/MIL-53(Al) and (5%Ce-20%Cu)/MIL-53(Al) for CO oxidation.

Fig.6 displays the CO oxidation activities for the (5%Ce-10%Cu)/MIL-53(Al), (5%Ce-20%Cu)/MIL-53(Al) and (5%Ce-5%Cu)/MIL-53(Al), with corresponding 100% conversion temperatures at 75, 83 and 85 °C respectively, but the temperature for 100% oxidation of CO on Cu/MIL-53(Al) is located at 300 °C. Ye and Liu^[31] reported that MOF-Cu[Cu₃(BTC)₂] could be used as catalysts for CO oxidation, with 100% conversion at 220-240 °C. Tan *et al.*^[32] reported that the temperature for 100% oxidation of CO on MOF-Co[Co₃(BTC)₂·12H₂O] at 150-160 °C. Obviously, the above three (Ce-Cu)/MIL-53(Al) catalysts display excellent activities, which is far better than that of Cu/MIL-53(Al) catalyst and previous reports^[1-3, 31, 32]. We

can reasonably envision that doping of Ce-Cu cations facilitates defect formation within the MIL-53(Al) lattice by generating lattice strain, which eventually improves the extrinsic surface defects, resulting in superior CO oxidation performance. The cerium doped copper nanoparticles resulting from the three dimensional porous structure of MIL-53(Al), the high specific surface area of MIL-53(Al) and the synergistic catalysis between cerium and copper are beneficial to increase the superior catalytic activity, which is consistent with previous literature reports^[33,34].

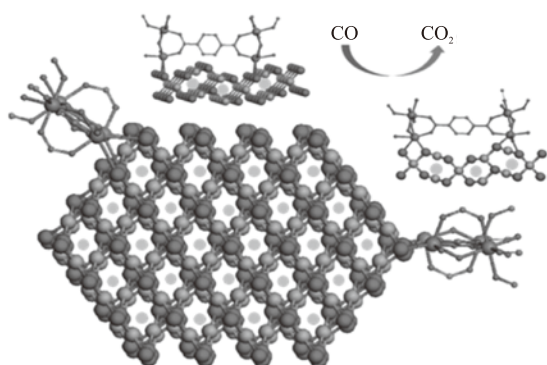


Fig.7 Schematic diagrams of dispersion of Ce doped CuO nanoparticles on the MIL-53(Al) carrier, ●, ○, ●, ● and ● represent the Ce, O, Cu, Al and C atoms, respectively

Fig.7 displays the calculated structure of cerium doped copper nano-particles (NPs) dispersed in MIL-53(Al). It is noticeable that the CuO NPs which were located in the center of a four member ring, consisted of four O atoms belonging to two adjacent Al nodes interacting with the O atoms of the MIL-53(Al), where the organic framework, such as benzene, virtually serves as spectator. Structurally, the high activity of the catalyst is mainly attributed to the relatively large specific surface area of the (Ce-Cu) NPs, which originated from the small particle size in the MOFs and the strong synergistic effect between copper and cerium. This configuration is pretty beneficial to much more exposure of the CuO NPs than the saturation of CuO embedded in the carrier, which is easily accessible for CO and O₂ gases due to the abundant pores and channels in the MOFs. Furthermore, the strong interaction between (Ce-Cu) NPs and MOFs increased the thermal and catalytic stabilities of the catalyst, which is sharply improved compared with the reported MOFs-based catalysts^[2,3,20]. In conclusion, the analyses indicate that the unique copper spatial confinement in the obtained solids minimizes catalyst deactivation, resulting in high activity and stable operation.

4 Conclusions

In summary, (Ce-Cu)/MIL-53(Al) catalyst has been prepared by impregnation method, serving as a catalyst with high activity for CO oxidation. Due to the high surface area, excellent stability, highly dispersed nanoparticles, strong synergistic effect between cerium and copper, (Ce-Cu)/MIL-53(Al) displays excellent activity in CO oxidation application, with 100% conversion at 75-85 °C, which is better than that of previous reports. This simple design strategy opens the door to the controlled pattern of highly dispersed and stable metal nanoparticles in porous matrices, one of the major challenges in MOF-materials and CO catalytic oxidation. The Ce doped Cu nanoparticles supported on MIL-53(Al) can be readily implemented in industry and provides a commercially feasible choice for CO oxidation reaction at low temperature and with high activity.

Acknowledgements

The authors thank the Key Laboratory of Catalysis and Materials Science of the State Ethnic Affairs Commission & Ministry of Education, Hubei Province, South-Central University for Nationalities for their measurement.

References

- [1] Tan H Y, Wu J P. Performance of a Metal-organic Framework MIL-53(Al)-Supported Cobalt Catalyst in the CO Catalytic Oxidation Reaction[J]. *Acta Phys.-Chim. Sin.*, 2014, 30: 715-722
- [2] Jiang H L, Liu B, Akita T, *et al.* Au@ ZIF-8: CO Oxidation over Gold Nanoparticles Deposited to Metal-organic Framework[J]. *J. Am. Chem. Soc.*, 2009, 131: 11 302-113 03
- [3] Liang Q, Zhao Z, Liu J, *et al.* Pd Nanoparticles Deposited on Metal-organic Framework of MIL-53(Al): an Active Catalyst for CO Oxidation[J]. *Acta Phys.-Chim. Sin.*, 2014, 30: 129-134
- [4] Zhao X, Xiao B, Fletcher A J, *et al.* Hysteretic Adsorption and Desorption of Hydrogen by Nanoporous Metal-organic Frameworks[J]. *Science*, 2004, 306: 1 012-1 015
- [5] Chae H K, Siberio-Pérez D Y, Kim J, *et al.* A Route to High Surface Area, Porosity and Inclusion of Large Molecules in Crystals[J]. *Nature*, 2004, 427: 523-527
- [6] Feng P, Bu X, Stucky G D. Hydrothermal Syntheses and Structural Characterization of Zeolite Analogue Compounds Based on Cobalt Phosphate[J]. *Nature*, 1997, 388: 735-741
- [7] Lu Y, Tonigold M, Bredenkötter B, *et al.* A Cobalt (II)-containing Metal-organic Framework Showing Catalytic Activity in Oxidation Reactions[J]. *Z. Anorg. Allg. Chem.*, 2008, 634: 2 411-2 417
- [8] Jiang D, Mallat T, Meier D M, *et al.* Copper Metal-organic Framework: Structure and Activity in the Allylic Oxidation of Cyclohexene

- with Molecular Oxygen[J]. *J. Cater.*, 2010, 270: 26-33
- [9] Schlichte K, Kratzke T, Kaskel S. Improved Synthesis, Thermal Stability and Catalytic Properties of the Metal-organic Framework Compound $\text{Cu}_3(\text{BTC})_2$ [J]. *Mirpopor. Mesopor. Mat.*, 2004, 73: 81-88
- [10] Huang Y, Liu S, Lin Z, et al. Facile Synthesis of Palladium Nanoparticles Encapsulated in Amine-functionalized Mesoporous Metal-organic Frameworks and Catalytic for Dehalogenation of Aryl Chlorides[J]. *J. Cater.*, 2012, 292: 111-117
- [11] Yaghi O, Li H, Groy T. Construction of Porous Solids from Hydrogen-bonded Metal Complexes of 1, 3, 5-benzenetricarboxylic Acid[J]. *J. Am. Chem. Soc.*, 1996, 118(38): 9 096-9 101
- [12] Jiang D, Mallat T, Krumeich F, et al. Polymer-assisted Synthesis of Nanocrystalline Copper-based Metal-organic Framework for Amine Oxidation[J]. *Catal. Commun.*, 2011, 12: 602-605
- [13] Ishida T, Nagaoka M, Akita T, et al. Deposition of Gold Clusters on Porous Coordination Polymers by Solid Grinding and Their Catalytic Activity in Aerobic Oxidation of Alcohols[J]. *Chem. Eur. J.*, 2008, 14: 8 456-8 460
- [14] Brown K, Zolezzi S, Aguirre P, et al. $[\text{Cu}(\text{H}(\text{btc})(\text{bipy}))_\infty]$: a Novel Metal Organic Framework (MOF) as Heterogeneous Catalyst for the Oxidation of Olefins[J]. *Dalton Trans.*, 2009, 10: 1 422-1 427
- [15] Tonigold M, Lu Y, Bredenkötter B, et al. Heterogeneous Catalytic Oxidation by MFU-1: A Cobalt (II)-containing Metal-organic Framework[J]. *Angew Chem. Int. Ed.*, 2009, 48: 7 546-7 550
- [16] Marx S, Kleist W, Baiker A. Synthesis, Structural Properties, and Catalytic Behavior of Cu-BTC and Mixed-linker Cu-BTC-PyDC in the Oxidation of Benzene Derivatives[J]. *J. Cater.*, 2011, 281: 76-87
- [17] Sun C Y, Liu S X, Liang D D, et al. Highly Stable Crystalline Catalysts Based on a Microporous Metal-organic Framework and Polyoxometalates[J]. *J. Am. Chem. Soc.*, 2009, 131: 1 883-1 888
- [18] Wee L H, Bajpe S R, Janssens N, et al. Convenient Synthesis of $\text{Cu}_3(\text{BTC})_2$ Encapsulated Keggin Heteropolyacid Nanomaterial for Application in Catalysis[J]. *Chem. Commun.*, 2010, 46: 8 186-8 188
- [19] Qiu W G, Wang Y, Li C Q, et al. Effect of Activation Temperature on Catalytic Performance of CuBTC for CO Oxidation[J]. *Chin. J. Catal.*, 2012, 33: 986-992
- [20] Tan Z D, Tan H Y, Shi X Y, et al. Metal-organic Framework MIL-53 (Al)-supported Copper Catalyst for CO Catalytic Oxidation Reaction[J]. *Inorg Chem. Commun.*, 2015, 61: 128-131
- [21] Kuo C H, Li W, Song W, et al. Facile Synthesis of Co_3O_4 @ CNT with High Catalytic Activity for CO Oxidation under Moisture-rich Conditions[J]. *ACS Appl. Mater. Inter.*, 2014, 6: 11 311-11 317
- [22] Lou Y, Cao X M, Lan J, et al. Ultralow-temperature CO oxidation on an In_2O_3 - Co_3O_4 Catalyst: a Strategy to Tune CO Adsorption Strength and Oxygen Activation Simultaneously[J]. *Chem. Commun.*, 2014, 50: 6 835-6 838
- [23] Song W, Poyraz A S, Meng Y, et al. Mesoporous Co_3O_4 with Controlled Porosity: Inverse Micelle Synthesis and High-Performance Catalytic CO Oxidation at -60°C [J]. *Chem. Mater.*, 2014, 26: 4 629-4 639
- [24] Xiao J, Wan L, Wang X, et al. Mesoporous Mn_2O_3 -CoO Core-shell Spheres Wrapped by Carbon Nanotubes: a High Performance Catalyst for the Oxygen Reduction Reaction and CO Oxidation[J]. *J. Mater. Chem. A*, 2014, 2: 3 794-3 800
- [25] Díaz A A, Cecilia J, Santos L D, et al. Characterization and Performance in Preferential Oxidation of CO of CuO-CeO₂ Catalysts Synthesized using Polymethyl Metacrylate (PMMA) as Template[J]. *Int. J. Hydrogen Energy*, 2015, 40: 11 254-11 260
- [26] Zeng S H, Zhang W L, Śliwa M, et al. Comparative Study of CeO₂/CuO and CuO/CeO₂ Catalysts on Catalytic Performance for Preferential CO Oxidation[J]. *Int. J. Hydrogen Energy*, 2013, 38: 3 597-3 605
- [27] Baneshi J, Haghighi M, Jodeiri N, et al. Homogeneous Precipitation Synthesis of CuO-ZrO₂-CeO₂-Al₂O₃ Nanocatalyst used in Hydrogen Production via Methanol Steam Reforming for Fuel Cell Applications[J]. *Energy Convers. Manage.*, 2014, 87: 928-937
- [28] Qi L, Yu Q, Dai Y, et al. Influence of Cerium Precursors on the Structure and Reducibility of Mesoporous CuO-CeO₂ Catalysts for CO Oxidation[J]. *Appl. Catal. B.*, 2012, 119: 308-320
- [29] Reyes-Carmona Á, Arango-Díaz A, Moretti E, et al. CuO/CeO₂ Supported on Zr doped SBA-15 as Catalysts for Preferential CO Oxidation (CO-PROX)[J]. *J. Power Sources*, 2011, 196: 4 382-4 387
- [30] Tang C, Sun J, Yao X, et al. Efficient Fabrication of Active CuO-CeO₂/SBA-15 Catalysts for Preferential Oxidation of CO by Solid State Impregnation[J]. *Appl. Catal. B*, 2014, 146: 201-212
- [31] Ye J Y, Liu C J. Cu₃(BTC)₂: CO Oxidation over MOF Based Catalysts[J]. *Chem. Commun.*, 2011, 47: 2 167-2 169
- [32] Tan H Y, Liu C, Yan Y F. Simple Preparation of Crystal $\text{Co}_3(\text{BTC})_2 \cdot 12\text{H}_2\text{O}$ and Its Catalytic Activity in CO Oxidation Reaction[J]. *J. Wuhan University of Technology-Mater. Sci. Ed.*, 2015, 30: 71-75
- [33] Li T Y, Xiang G L, Zhuang J, et al. Enhanced Catalytic Performance of Assembled Ceria Necklace Nanowires by Ni Doping[J]. *Chem. Commun.*, 2011, 47: 6 060-6 061
- [34] Yu Q, Wu X X, Tang C J, et al. Textural, Structural, and Morphological Characterizations and Catalytic Activity of Nanosized CeO₂-MO_x (M= Mg²⁺, Al³⁺, Si⁴⁺) Mixed Oxides for CO Oxidation[J]. *J. Colloid Interface Sci.*, 2011, 354: 341-352